Inorg. Chem. **2006**, *45*, 5538–5551

Conformationally Gated Photoinduced Processes within Photosensitizer–Acceptor Dyads Based on Osmium(II) Complexes with Triarylpyridinio-Functionalized Terpyridyl Ligands: Insights from Theoretical Analysis

Philippe P. Lainé,*,† Frédérique Loiseau,‡ Sebastiano Campagna,‡ Ilaria Ciofini,§ and Carlo Adamo*,§

Contribution from the Laboratoire de Chimie et Biochimie Pharmacologiques et Toxicologiques, CNRS UMR-8601, Université René Descartes, 45 rue des Saints Pères, F-75270, Paris Cedex 06, France, Università di Messina, Dipartimento di Chimica Inorganica, Chimica Analitica e Chimica Fisica, Via Sperone 31, I-98166 Messina, Italy, and Laboratoire d'Électrochimie et Chimie Analytique, CNRS UMR-7575, École Nationale Supérieure de Chimie de Paris, 11 rue Pierre et Marie Curie, F-75231 Paris Cedex 05, France

Received April 21, 2006

A theoretical analysis, based on density functional theory, has been carried out to study photoinduced processes within a recently experimentally characterized (Lainé, P. P.; Bedioui, F.; Loiseau, F.; Chiorboli, C.; Campagna, S. *J. Am. Chem. Soc.* **2006**, http://dx.doi.org/10.1021/ja058357w.) series of Os(II) bis-tpy complexes (tpy = 2,2′:6′2″-terpyridine) functionalized by 2,4,6-triarylpyridinium groups, TP^+. These dyad systems, designed to produce a charge-separated state (CSS) upon light excitation, are made up of a photosensitizer unit (P, the metal complex) and a tunable acceptor unit (A, the TP^+). A full ab initio characterization of the electronic and structural properties of the lowest-lying triplet excited states, as well as of the CSS, allowed for a complete rationalization of the photoinduced processes taking place within the dyads. Among salient insights, theory allowed (i) substantiation of the inner P structural planarization as the relaxation mode of the MLCT states, (ii) confirmation of the existence of a ligand-centered triplet excited state (^{3}LC) shown to essentially involve the nitro substituent of A (TP^+-NO_2) and lying very close in energy to the P-centered ^{3}MLCT state, and (iii) a demonstration that the energy of the ^{3}LC level is independent of intercomponent tilt angle (θ_1). On this basis, the occurrence of a reversible electronic energy transfer between the ^{3}MLCT and the ^{3}LC states could be substantiated and shown to depend on the intramolecular conformation represented by θ_1, which actually governs their electronic coupling (essentially via the degree of intercomponent conjugation). These computational issues were checked against experimental data already available and the results of a specifically undertaken photophysical study. Finally, CSS formation has been confirmed by studying the spin density patterns of reduced nitro-derivatized dyads. Taken together, these findings accurately account for the different excited-state behaviors of the dyads as a function of the level of structural restriction of their intercomponent conformation (and related amplitude for torsional fluctuations), thus providing theoretical evidence of *conformationally gated photoinduced electron- and energy-transfer processes*.

1. Introduction

Supramolecular[2] and bioinorganic[3] photochemistry are closely related research fields which have a share in the advancement of the affiliated topics[4] of artificial photosynthesis and molecular electronics (nanosciences). In this interdisciplinary context, understanding how photoinduced phenomena can be "gated" by intramolecular conformation

* To whom correspondence should be addressed. E-mail: philippe.laine@univ-paris5.fr (P.P.L.); carlo-adamo@enscp.fr (C.A.).
† Université René Descartes.
‡ Università di Messina.
§ École Nationale Supérieure de Chimie de Paris (ENSCP).

(1) For Part 1, see: Lainé, P. P.; Bedioui, F.; Loiseau, F.; Chiorboli, C.; Campagna, S. *J. Am. Chem. Soc.* **2006**, http://dx.doi.org/10.1021/ja058357w.
(2) (a) Balzani, V.; Juris, A.; Venturi, M.; Campagna, S.; Serroni, S. *Chem. Rev.* **1996**, *96*, 759−833. (b) Balzani, V.; Scandola, F. *Supramolecular Photochemistry*; Ellis Horwood: Chichester, U.K., 1991. (c) Balzani, V.; Moggi, L.; Scandola, F. In *Supramolecular Photochemistry*; Balzani, V., Ed; D. Reidel Publishing Co.: Dordrecht, The Netherlands, 1987; pp 1−28.

10.1021/ic060679t CCC: $33.50
Published on Web 06/08/2006

when intricately *entangled states* are present is a long-standing issue of importance.[5−7] Indeed, given that molecular geometry can be controlled by external stimuli,[8] the design of novel photochemical molecular devices (PMDs)[2] could therefore be envisioned. The study of multicomponent systems composed of functional subunits acting in either electron (ET) or energy (EnT) transfers and showing potentially fully conjugated rigid rodlike architectures is expected to provide insights into this challenging problem.

Most of PMDs presently examined have been designed to transiently convert light energy into "redox energy" by generating so-called charge-separated states (CSS). The strategy usually adopted to successfully achieve such a complex function consists of building molecular assemblies made of selected photoactive and redox-active subunits, preferably linearly arranged.[9] For these supermolecules, the control of intercomponent electronic coupling is a key point. The coupling has to remain weak[10] to favor hopping of the electrons (or holes) between predetermined intramolecular discrete states.[9,11] To this end, we[12,13] and others[14−20] have relied on the control of molecular structural properties,[21] according to the so-called "geometrical-decoupling" strategy.[12]

In the present work, we will focus on the *excited states* of two-component assemblies (dyads) consisting of an inorganic photosensitizer (P) covalently linked to an electron-acceptor unit (A). More precisely, P is a bis-2,2′:6′,2"-terpyridine (tpy) complex (denoted P0/M or P1/M, Chart 1) of 2nd and 3rd row d^6 transition metal dications (M = Ru^{2+} and Os^{2+}), and A is the chemically (and electronically) tunable triarylpyridinium group (TP^+, Chart 1).[12]

Chart 1. Chemical Structures and Corresponding Labels of Reference Model Acceptors (A_{Ref}) and Related Dyads

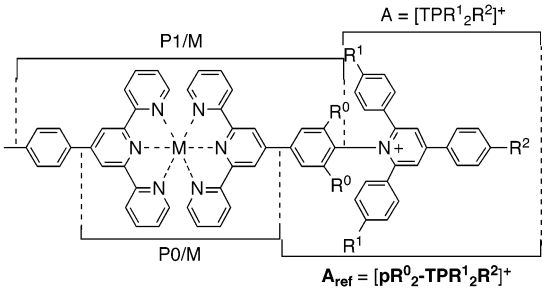

A_{ref}	Dyads (M = Os^{2+} (Ru^{2+}))		
ph-TPH_3^+	**2**	(**7**)	$R^0 = R^1 = R^2 = H$
xy-TPH_3^+	**3**	(**8**)	R^0 = Me and $R^1 = R^2 = H$
ph-$TPH_2(NO_2)^+$	**4**	(**9**)	$R^0 = R^1 = H$ and $R^2 = NO_2$
xy-$TPH_2(NO_2)^+$	**5**	(**10**)	R^0 = Me, R^1 = H and $R^2 = NO_2$

The photophysical behavior of the whole series of dyads represented in Chart 1 has been investigated in the related experimental study[1] together with that of reference photosensitizers, $[M(ttpy)_2]^{2+}$ (ttpy = 4′-*p*-tolyl-tpy, M = Os^{2+} (**1**) and Ru^{2+} (**6**)), which can be viewed as models for the P1/M parent component of the supermolecules (Chart 1).[1] The scope of the present theoretical work is however essentially limited to selected osmium(II) compounds (**1**, **2**, **4**, and **5**). Indeed, experimental studies[1] have shown that the targeted CSS, $*[P^+-A^-]$, can be formed only in osmium-based dyads **4** and **5**. It was also found that these two dyads behave differently. System **4** exhibits a long emission lifetime (174 ns) compared to that of **5** (870 ps), even though both species have very similar (and low) emission quantum yields. This difference has been attributed to an intervening reversible EnT process (equilibration) in excited dyad **4**, postulated to involve the ^{3}MLCT emitting state of P1/Os and a ligand-centered (LC) triplet state close in energy (even isoenergetic).

(3) Szacilowski, K.; Macyk, W.; Drzewiecka-Matuszek, A.; Brindell, M.; Stochel, G. *Chem. Rev.* **2005**, *105*, 2647−2694.
(4) Gust, D.; Moore, T. A.; Moore, A. L. *Acc. Chem. Res.* **2001**, *34*, 40−48.
(5) Osyczka, A.; Moser, C. C.; Daldal, F.; Dutton, L. *Nature* **2004**, *427*, 607−612.
(6) (a) Weiss, E. A.; Tauber, M. J.; Kelley, R. F.; Ahrens, M. J.; Ratner, M. A.; Wasielewski, M. R. *J. Am. Chem. Soc.* **2005**, *127*, 11842−11850. (b) Davis, W. B.; Ratner, M. A.; Wasielewski, M. R. *J. Am. Chem. Soc.* **2001**, *123*, 7877−7886.
(7) Brunschwig, B. S.; Sutin, N. *J. Am. Chem. Soc.* **1989**, *111*, 7454−7465.
(8) For recent examples, see: (a) (ion binding) Oike, T.; Kurata, T.; Takimiya, K.; Otsubo, T.; Aso, Y.; Zhang, H.; Araki, Y.; Ito, O. *J. Am. Chem. Soc.* **2005**, *127*, 15372−15373. Benniston, A. C.; Li, P.; Sams, C. *Tetrahedron Lett.* **2003**, *44*, 3947−3949. (b) (electric field) Troisi, A.; Ratner, M. A. *Nano Lett.* **2004**, *4*, 591−595. Derosa, P. A.; Guda, S.; Seminario, J. M. *J. Am. Chem. Soc.* **2003**, *125*, 14240−14241. (c) (light) Jousselme, B.; Blanchard, P.; Gallego-Planas, N.; Delaunay, J.; Allain, M.; Richomme, P.; Levillain, E.; Roncali, J. *J. Am. Chem. Soc.* **2003**, *125*, 2888−2889.
(9) (a) Baranoff, E.; Collin, J.-P.; Flamigni, L.; Sauvage, J.-P. *Chem. Soc. Rev.* **2004**, *33*, 147−155. (b) Dixon, I. M.; Collin, J.-P.; Sauvage, J.-P.; Barigelletti, F.; Flamigni, L. *Angew. Chem., Int. Ed.* **2000**, *39*, 1292−1295. (c) Collin, J.-P.; Gaviña, P.; Heitz, V.; Sauvage, J.-P. *Eur. J. Inorg. Chem.* **1998**, 1−14. (d) Barigelletti, F.; Flamigni, L.; Collin, J.-P.; Sauvage, J.-P. *Chem. Commun.* **1997**, 333−338. (e) Sauvage, J.-P.; Collin, J.-P.; Chambron, J.-C.; Guillerez, S.; Coudret, C.; Balzani, V.; Barigelleti, F.; De Cola, L.; Flamigni, L. *Chem. Rev.* **1994**, *94*, 993−1019.
(10) Balzani, V. *Tetrahedron* **1992**, *48*, 10443−10514.
(11) (a) Valásek, M.; Pecka, J.; Jindrich, J.; Calleja, G.; Craig, P. R.; Michl, J. *J. Org. Chem.* **2005**, *70*, 405−412. (b) Berlin, Y. A.; Hutchison, G. R.; Rampala, P.; Ratner, M. A.; Michl, J. *J. Phys. Chem. A* **2003**, *107*, 3970−3980.
(12) (a) Lainé, P.; Bedioui, F.; Amouyal, E.; Albin, V.; Berruyer-Penaud, F. *Chem.—Eur. J.* **2002**, *8*, 3162−3176. (b) Lainé, P.; Bedioui, F.; Ochsenbein, P.; Marvaud, V.; Bonin, M.; Amouyal, E. *J. Am. Chem. Soc.* **2002**, *124*, 1364−1377. (c) Lainé, P.; Amouyal, E. *Chem. Commun.* **1999**, 935−936.
(13) Lainé, P. P.; Ciofini, I.; Ochsenbein, P.; Amouyal, E.; Adamo, C.; Bedioui, F. *Chem.—Eur. J.* **2005**, *11*, 3711−3727.
(14) The scope of our discussion is mainly focused on inorganic assemblies and restricted to non-porphyrinic systems.
(15) (a) Benniston, A. C.; Harriman, A.; Li, P.; Patel, P. V.; Sams, C. A. *Phys. Chem. Chem. Phys.* **2005**, *7*, 3677−3679. (b) Benniston, A. C.; Harriman, A.; Li, P.; Sams, C. A.; Ward, M. D. *J. Am. Chem. Soc.* **2004**, *126*, 13630−13631. (c) Benniston, A. C.; Harriman, A.; Li, P.; Sams, C. A. *Phys. Chem. Chem. Phys.* **2004**, *6*, 875−877. (d) Benniston, A. C.; Harriman, A.; Li, P.; Sams, C. A. *Tetrahedron Lett.* **2003**, *44*, 4167−4169.
(16) Johansson, O.; Borgström, M.; Lomoth, R.; Palmblad, M.; Bergquist, J.; Hammarström, L.; Sun, L.; Åkermark, B. *Inorg. Chem.* **2003**, *42*, 2908−2918.
(17) Miller, S. E.; Lukas, A. S.; Marsh, E.; Bushard, P.; Wasielewski, M. R. *J. Am. Chem. Soc.* **2000**, *122*, 7802−7810 and references therein.
(18) (a) Ward, M. D. *Chem. Soc. Rev.* **1995**, 121−134. (b) Pierce, D. T.; Geiger, W. E. *Inorg. Chem.* **1994**, *33*, 373−381. (c) Dong, T.-Y.; Huang, C.-H.; Chang, C.-K.; Wen, Y.-S.; Lee, S.-L.; Chen, J.-A.; Yeh, W.-Y.; Yeh, A. *J. Am. Chem. Soc.* **1993**, *115*, 6357−6368. (d) Larson, S. *J. Am. Chem. Soc.* **1981**, *103*, 4034−4040. (e) Tanner, M.; Ludi, A. *Inorg. Chem.* **1981**, *20*, 2348−2350. (f) Fisher, H.; Tom, G. M.; Taube, H. *J. Am. Chem. Soc.* **1976**, *98*, 5512−5517.
(19) Tapolsky, G.; Duesing, R.; Meyer, T. J. *Inorg. Chem.* **1990**, *28*, 2285−2297.
(20) (a) Gourdon, A. *New. J. Chem.* **1992**, *16*, 953−957. (b) Woitellier, S.; Launay, J.-P.; Joachim, C. *Chem. Phys.* **1989**, *131*, 481−488. (c) Joachim, C.; Launay, J.-P. *Chem. Phys.* **1986**, *109*, 93−99.
(21) Harriman, A. *Angew. Chem., Int. Ed.* **2004**, *43*, 4985−4987.

Chart 2. Relevant Torsion Angles and Nomenclature[a]

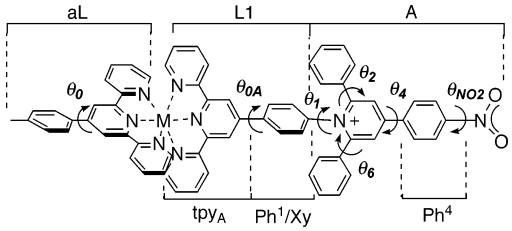

[a] Ph^1 becomes xy when R^0 = Me (cf. Chart 1).

The latter has not been directly and clearly identified at the experimental level, however. The equilibration is assumed to be in competition with thermodynamically favored intramolecular ET leading to CSS formation[1] as both processes originate from the same ^{3}MLCT level. As a result, phosphorescence emission of the photosensitizer within **4** is prolonged despite its very low quantum yield. In the case of **5**, no such equilibration takes place; instead, there is only intramolecular oxidative quenching of *P by A, leading to direct CSS formation.

Investigation conducted by ultrafast transient absorption spectroscopy (sub-picosecond time scale) also showed an increase in the absorption in the NIR region for the whole series (**1**−**5**) of complexes, which was attributed to a structural relaxation within the P1/Os component. This *planarization* has been postulated to occur about the torsion angle involving the P0/Os core and the linked phenyl ring, the building blocks of the P1/Os photosensitizer (Chart 1).

Although the experimental study of the whole series of complexes has provided a rather clear overall picture of the intramolecular photoinduced processes, still several issues of importance deserved to be further clarified. To this end and because of the nature of questions to be assessed, an ab initio (*from first principles)* theoretical approach is deemed to be a choice and proven method.[22] In particular, density functional theory (DFT) will be applied since it has been remarkably successful in the accurate evaluation of a variety of ground- and excited-state properties of large systems and, especially, of complexes containing transition metals.[23−25]

First, we will concentrate on the *equilibration process* postulated to explain the paradoxical emission properties measured for dyad **4** and its differences with respect to **5**.[1] Obviously, the main distinction between **4** and **5** stems from the level of conformational restriction around the θ_1 torsion angle (Chart 2), given that the ^{3}MLCT and CS states energy levels are roughly the same for both species.[1] For **5**, the presence of bulky methyl substituents (R^0) in the immediate vicinity of the P−A intercomponent linkage (Chart 1) is anticipated to lock the "geometrical decoupling", including that in the excited state, while conformational fluctuations are partially allowed in **4**, as experimentally inferred in ref 1. It is not clear, however, to what extent the twist angle determines the equilibration process in *[**4**] and *[**5**], reversible EnT is precluded in the latter case.

Beyond the *actual identity* of the equilibrated level (^{3}LC), which will be also established in the present work, the first question to be answered theoretically is related to the extent of its spatial expanse, in particular, to determine if the intercomponent bonding is concerned. From a mechanistic viewpoint, three different cases can be envisioned.

(i) The energy of the ^{3}LC-equilibrated state is controlled by θ_1, increasing from an almost isoenergetic position to a thermally inaccessible one with respect to that of the P1/Os-based ^{3}MLCT level on changing from *[**4**] to *[**5**].

(ii) The ^{3}LC energy remains unchanged regardless of θ_1, but the ^{3}LC state becomes inaccessible in **5** because of the loss of intercomponent conjugation. In other words, the electronic coupling between the two isoenergetic levels is no longer sufficient to allow equilibration within **5**, while is apparently sufficient in **4** thanks to the conformational fluctuations.

(iii) Both the energy of the ^{3}LC level and the electronic coupling of the latter with the ^{3}MLCT level are concomitantly altered as described above (i and ii).

Theoretical issues, which favor case ii above, were checked against the outcomes of a photophysical study of selected references species.

Second, we will examine the phenomenon of *planarization* upon charge transfer (CT), experimentally inferred for MLCT states.[1,13,26−32] The aim of the present study is to further substantiate this geometrical aspect by theoretical means before investigating its importance in other photoproduced states (namely ^{3}LC and CS states). Particular attention will be paid to the θ_{0A} and θ_1 twist angles involving the bridging (B) phenyl (Ph^1) or xylyl (Xy) aryl fragment (Chart 2), the function of which is actually dual. Indeed, B fully partakes of both components P (antenna effect) and A (as an influential *N*-pyridinio substituent),[1,12a] and at the same time, B also plays the role of a spacer between the cores of both P (that is P0/Os) and A (pyridinium ring). Basically, B should be considered to be a full functional element in the same capacity as P and A, with its own electronic identity and correlated spectral signature.[12a,22] Conformational changes will be analyzed in light of the spin-density patterns of the triplet excited states and of the charge partitioning (i.e., CSS formation) within reduced species to substantiate the postulated correlation. Also, the backward effects of the

(22) Ciofini, I.; Lainé, P. P.; Bedioui, F.; Adamo, C. *J. Am. Chem. Soc*. **2004**, *126*, 10763−10777.
(23) Koch, W.; Holthausen, M. C. *A Chemist's Guide to Density Functional Theory*; Wiley-VCH: Weinheim, Germany, 2000.
(24) Adamo, C.; di Matteo, A.; Barone, V. *Adv. Quantum Chem*. **1999**, *36*, 45−75.
(25) Burke, K.; Perdew, J. P.; Wang, Y. In *Electronic Density Functional Theory: Recent Progress and New Derivations*; Dobson, J. F., Vignale, G., Das, M. P., Eds.; Plenum Press: New York, 1997.
(26) Busby, M.; Liard, D. J.; Motevalli, M.; Toms, H.; Vlcek, A., Jr. *Inorg. Chim. Acta* **2004**, *357*, 167−176.
(27) Liard, D. J.; Busby, M.; Farrell, I. R.; Matousek, P.; Towrie, M.; Vlcek, A., Jr. *J. Phys. Chem. A* **2004**, *108*, 556−567.
(28) Damrauer, N. H.; McCusker, J. K. *J. Phys. Chem. A* **1999**, *103*, 8440−8446.
(29) Damrauer, N. H.; Weldon, B. T.; McCusker, J. K. *J. Phys. Chem. A* **1998**, *102*, 3382−3397.
(30) Damrauer, N. H.; Boussie, T. R.; Devenney, M.; McCusker, J. K. *J. Am. Chem. Soc*. **1997**, *119*, 8253−8268.
(31) Chen, P.; Curry, M.; Meyer, T. J. *Inorg. Chem*. **1989**, *28*, 2271−2280.
(32) Berg-Brennan, C.; Subramanian, P.; Absi, M.; Stern, C.; Hupp, J. T. *Inorg. Chem*. **1996**, *35*, 3719−3722.

structural *relaxation* toward planarity on the spin-density redistribution will be examined as fluctuation of the structure conformation is anticipated to result in variations of pivotal intercomponent electronic couplings.[15a,19,33]

In the course of the present study, we will also substantiate CSS formation at the theoretical level, discuss the influence of the nitro group, and clarify the role of R^0 substituents which, in addition to *structural* aspects,[29] may have a beneficial contribution, as electron-donating inductive groups, to the "insulation capacity" of the spacer.[17]

It is worthwhile to underline that the knowledge of the very nature of determining factors that govern photoinduced processes at the intramolecular level when multiple channels are potentially available (and operative) in the excited state, is a key issue when planning specialized PMDs relying on ET, EnT, or both.

2. Experimental Section

All compounds were synthesized and fully characterized as described in refs 1 and 12b.

2.1. Computational Methods. All calculations were carried out using Gaussian03.[34] A hybrid Hartree−Fock/density functional model, referred to as PBE0, was used.[35] This approach was obtained by casting the PBE exchange and correlation functional[36] in a hybrid DFT/HF scheme, where the HF/DFT exchange ratio is fixed a priori to 1/4.[37]

In the case of the open-shell systems, unrestricted calculations were performed, and spin contamination, monitored by the expectation value of S^2, was found to be negligible.

A double-ζ quality LANL2 basis[38] and corresponding pseudopotentials for the metal atoms[39] were used for all atoms both for the structural optimizations and the calculation of the electronic properties. Such a level of theory (DFT + LANL2DZ basis set) has previously been successfully applied in a few works concerning the structure, spectroscopic properties, and reactivity of organometallic systems.[40,41]

The molecular structure of all systems was fully optimized without symmetry constraints. All triplet states were computed (and structurally relaxed) using a ΔSCF approach.[41b,42]

When spin density patterns and their integrated values (atomic spin population, ASP) are reported, we always refer to the Mulliken partition scheme with the polarization of the core of the Os metal being neglected.

2.2. Photophysical Characterizations. For steady-state luminescence measurements, a Jobin Yvon-Spex Fluoromax 2 spectrofluorimeter, equipped with a Hamamatsu R3896 photomultiplier, was used, and the spectra were corrected for photomultiplier response using a program purchased with the fluorimeter. For the luminescence lifetimes, an Edinburgh OB 900 time-correlated single-photon-counting spectrometer was used in the nanosecond range. As excitation sources, a Hamamatsu PLP 2 laser diode (59 ps pulse width at 408 nm) and nitrogen discharge (pulse width, 2 ns at 337 nm) were employed.

3. Results and Discussion

The ($S_0 \rightarrow S_1/S_n$) and ($S_0 \rightarrow T_1$) MLCT electronic transitions can be considered to be elementary events on the way to fully developed CSS formation. Basically, primary MLCT and the ensuing CS states are very similar in nature, being mainly differentiated in terms of electron−hole coupling in relation to their spatial separation. Such a difference is reflected by the fact that a *transition moment* no longer makes sense for the fully developed CS (and is no longer defined accordingly). In general, it is therefore worth referring to *photoinduced* (i.e., stepwise) ET processes for CS formation versus *direct optical* ET for MLCT transitions.[43] Consequently, in the present work, the primary excited states, related to the early events following light excitation of the photosensitizer, are theoretically analyzed by computing the features of the related excited states (section 3.1). On the other hand, the ensuing CS states are preferably assessed by analyzing the ground state of the corresponding monoreduced species (section 3.3). In other words, the component "electron" of the photodissociated initial pair (exciton) is considered and treated regardless of its formally related hole (metal-centered). In such a way, the MLCT states investigated in section 3.1 as true spectroscopic triplets were also re-examined.

For charge redistribution upon light excitation, we preferably discussed the spin-density patterns and their integrated values (atomic spin population, ASP), rather than on the shape of the SOMO or LUMO orbitals themselves; thus, the non-negligible contribution of spin polarization originating from inner-lying electrons is taken into account.[13,22,44] Spin density patterns were also computed to investigate electronic reorganization within the triplet states of the various inorganic species.

(33) Cotlet, M.; Masuo, S.; Luo, G.; Hofkens, J.; Van der Auweraer, M.; Verhoeven, J.; Müllen, K.; Xie, X. S.; De Schryver, F. *Proc. Natl. Acad. Sci. U.S.A.* **2004**, *101*, 14343−14348.
(34) Frisch, M. J.; Trucks, G. W.; Schlegel, H. B.; Scuseria, G. E.; Robb, M. A.; Cheeseman, J. R.; Montgomery, J. A., Jr.; Vreven, T.; Kudin, K. N.; Burant, J. C.; Millam, J. M.; Iyengar, S. S.; Tomasi, J.; Barone, V.; Mennucci, B.; Cossi, M.; Scalmani, G.; Rega, N.; Petersson, G. A.; Nakatsuji, H.; Hada, M.; Ehara, M.; Toyota, K.; Fukuda, R.; Hasegawa, J.; Ishida, M.; Nakajima, T.; Honda, Y.; Kitao, O.; Nakai, H.; Li, X.; Knox, J. E.; Hratchian, H. P.; Cross, J. B.; Adamo, C.; Jaramillo, J.; Gomperts, R.; Stratmann, R. E.; Cammi, R.; Pomelli, C.; Ochterski, J.; Ayala, P. Y.; Morokuma, K.; Hase, W. L.; Salvador, P.; Dannenberg, J. J.; Zakrzewski, V. G.; Dapprich, S.; Daniels, A. D.; Strain, M. C.; Farkas, O.; Malick, D. K.; Rabuck, A. D.; Raghavachari, K.; Foresman, J. B.; Ortiz, J. V.; Cui, Q.; Baboul, A. G.; Clifford, S.; Cioslowski, J.; Stefanov, B. B.; Liu, G.; Liashenko, A.; Piskorz, P.; Komaromi, I.; Martin, R. L.; Fox, D. J.; Keith, T.; Al-Laham, M. A. C.; Peng, Y.; Nanayakkara, A.; Challacombe, M.; Gill, P. M. W.; Johnson, B.; Chen, W.; Wong, M. W.; Gonzalez, C.; Pople, J. A. *Gaussian Development Version*, revision B.05; Gaussian, Inc.: Pittsburgh, PA, 2003.
(35) Adamo, C.; Barone, V. *J. Chem. Phys.* **1999**, *110*, 6158−6170.
(36) Perdew, J. P.; Burke, K.; Ernzerhof, M. *Phys. Rev. Lett.* **1996**, *77*, 3865−3868.
(37) Adamo, C.; Barone, V. *Chem. Phys. Lett.* **1997**, *274*, 242−250.
(38) Dunning, T. H., Jr.; Hay, P. J. In *Modern Theoretical Chemistry*; Schaefer, H. F., III, Ed.; Plenum: New York, 1976; pp 1−28.
(39) Hay, J.; Wadt, W. R. J. *Chem. Phys.* **1985**, *82*, 299−310.
(40) (a) Boulet, P.; Chermette, H.; Daul, C. A.; Gilardoni, F.; Rogemond, F.; Weber, J.; Zuber, G. *J. Phys. Chem. A* **2001**, *105*, 885−894. (b) Boulet, P.; Chermette, H.; Weber, J. *Inorg. Chem.* **2001**, *40*, 7032−7039.
(41) (a) Ciofini, I.; Hazebroucq, S.; Joubert, L.; Adamo, C. *Theor. Chem. Acc.* **2004**, *111*, 188−195. (b) Ciofini, I.; Daul, C.; Adamo, C. *J. Phys. Chem. A.* **2003**, *107*, 11182−11190.
(42) Guillemoles, J.-F.; Barone, V.; Joubert, L.; Adamo, C. *J. Phys. Chem. A* **2002**, *106*, 11354−11360.
(43) In some cases, direct optical ET can lead to the formation of the CS state; see ref 22.
(44) Polson, M.; Ravaglia, M.; Fracasso, S.; Garavelli, M.; Scandola, F. *Inorg. Chem.* **2005**, *44*, 1282−1289.

Table 1. Computed ASP for the Relaxed Lowest-Lying Triplet States of Various Complexes (in fraction of electrons, sum = 2) Together with Related Triplet-to-Singlet (ground state, S_0) Nonadiabatic Relaxation Energy (eV)[a]

	*[1]	*[2]	*[4]		*[5]
	T_1	T_1	T_1	T_2	T_1
Os	**0.888**	**0.880**	**0.877**	**0.000_4**	**0.860**
tpy_A	0.529×2	0.950	1.025	0.000	0.790
Ph^1/Xy	0.027×2	0.080	0.085	0.020	0.030
L1	**0.556×2**	**1.030**	**1.110**	**0.020**	**0.820**
pyridinium		−0.002	0.003	0.100	0.002
Ph^4		0.000	0.000	0.130	0.000
NO_2			0.000	1.750	0.000
A		**0.003**	**0.003**	**1.980**	**0.002**
aL[b]	*c*	**0.087**	**0.010**	**0.000**	**0.318**
$E(T \rightarrow S_0)_{calcd}$	1.884	1.703	1.710	1.869_5	1.753
$E(T_1 \rightarrow S_0)_{exptl}$[d]	1.719	1.708	1.710		1.701

[a] Complex moieties (first column) are labeled as in Chart 2. [b] aL stands for ttpy ancillary ligand. [c] Refer to spin density located on L1. [d] Experimental value measured in deaerated frozen BuCN matrix at 77 K (/eV); see ref 1.

3.1. Early Stages of Photoinduced Processes: Theoretical Analysis. Processes relevant to the occurrence of intramolecular ET to CSS formation, such as the postulated planarization (with respect to the θ_{0A} angle, Chart 2), were experimentally found to take place within the first 2 ps after the laser pulse excitation.[1] With the inorganic photosensitizer as the primary electron donor and intersystem crossing ($S_1 \rightarrow T_1$) being achieved within ca. 300 fs,[45] we calculated the electron redistribution and associated structural relaxation for the *thermalized triplet* excited states.[46]

3.1.1. Electronic Excitation Patterns. Spin-Density Calculations and the Occurrence of Unexpected Triplet States. Computed ASP distributions for the lowest triplet states of **1**, **2**, **4**, and **5** are collected in Table 1. As expected, the lowest-lying triplet state (T_1) is MLCT in nature, in agreement the experimental paper.[1] Interestingly, it appears that another triplet state (T_2) is close in energy to the T_1, at least in the case of nitro-derivatized dyad **4**. Figure 1a−e illustrates the spin density patterns of computed triplets T_1 and T_2, the latter being specifically discussed in section 3.1.3.

Even though the P1/Os units are embedded within dyads, the ASPs suggest that the two unpaired electrons of T_1 are confined in the P1/Os component. Moreover, the ASP of the metal remains almost unchanged (ca. 44%), regardless of the P1/Os being isolated in the parent photosensitizer (**1**) or embedded in the dyad systems. As a consequence, the complementary contribution to ASP of T_1 related to the odd electron transferred on the tpy ligands remains unchanged for the whole series of compounds. It remains nonetheless that, when present, the TP^+ group is found to draw spin density located on the organic part of P1/Os toward the pyridinium ring of L1 (Figure 1b and c). ASP, located on the corresponding ancillary ttpy ligand (aL), is thus found to decrease in proportion by ca. 84 and 98% on going from **1** to dyads **2** and **4**, respectively. Hence, the directional character of the (ML)CT state is enhanced accordingly. Interestingly, it appears that the balance of ASP between the derivatized tpy (L1) and aL ligand becomes sharply different (Table 1, Figure 1c and e), on changing from **4** to **5**. In the case of **5**, the decrease of ASP on the aL ligand is only 43% (vs 98% for **4**), with respect to **1**, which might be attributed to the presence of methyl R^0 substituents on the L1 counterpart. In this regard, one can note a significant decrease of ca. 23% on average of the ASP located on the L1 fragment (the tpy moiety and the aryl spacer) on going from dyads **2** and **4** to complex **5**. Also, it is found that the spatial extension of the ^{3}MLCT state is larger within **4** than within **5**, as can be seen in Figure 1c and e. These differences are also indicative of a possible electronic contribution of the methyl groups of the spacer. However, at this stage, it is not clear to what extent an electronic contribution of the methyl groups of the xylyl spacer (in **5**) comes into play in addition to the purely structural effects.

These findings, taken together, are consistent with the experiment.[1] For ground-state properties, the conservation of the balance of the ASP partition between M and L within P1/Os throughout the whole series of compounds parallel the corresponding electrochemical behavior and, more specifically, the observed constant redox potential for the oxidation of the metal center within the P1/Os unit.[1] For the excited-states, the conserved ASP balance complies with the observed constancy of the ^{3}MLCT-based emission energy throughout the whole series of dyads. In summary, these trends reflect the weak intercomponent coupling in both the ground and excited states.

3.1.2. Structural Reorganization: Planarization of the Triplet States. Computed structural features of the triplet states for various complexes are gathered in Table 2.

Apparently, the main geometrical difference between **4** and **5** resides in the value of the θ_1 torsion angle, which is larger in the latter case by ca. 10° in the ground (S_0) and excited (T_1 and T_2) states. This computational outcome is indicative of the possibility for a larger electron delocalization within **4**, whose conformational motion is only *restrained*, than within **5**, for which geometrical decoupling is *constrained* (even locked). This theoretical finding confirms the validity of our engineering approach to *geometrical decoupling in the excited state*, based on the insertion of a bulky substituent at the R^0 positions (Chart 1).

An inspection of Table 2 allows us to identify two types of structural relaxation toward planarity for dyads in the excited states. One is the expected inner-photosensitizer planarization around θ_0 and θ_{0A}. These angles are modified with different amplitudes, the latter being the most affected. This planarization is hardly reproduced both for **1** and P1/Os embedded within **2**, compared to that of other more-polarized dyads.[47] The second type of planarization is found to occur within the acceptor unit, more specifically and solely concerning θ_4.

When the spin-density patterns (Table 1) and the variation of structural features on going from the ground to excited

(45) Damrauer, N. H.; Cerullo, G.; Yeh, A.; Boussie, T. R.; Shank, C. V.; McCusker, J. K. *Science* **1997**, *275*, 54−57.
(46) Vlcek, A., Jr. *Coord. Chem. Rev.* **2000**, *200*−*202*, 933−977.
(47) For **1**, see section 3.3.2. Notice that the same miscalculation of planarization has been found for the $[(4t\text{-dppy})Ir(ttpy)]^+$ (4t-dppy is 2,6-diphenyl-4-(4-tolyl)-pyridine) affiliated iridium(III) cyclometalated complex, investigated at a similar level of theory.[44]

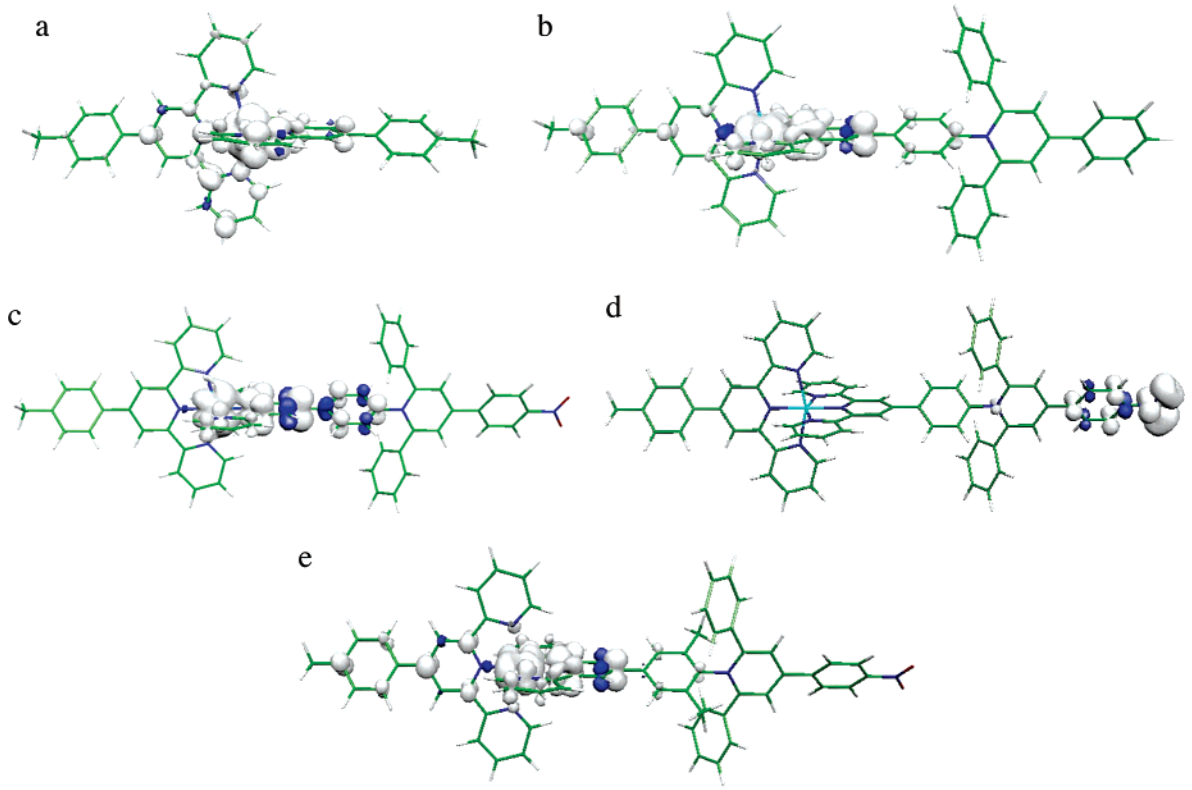

Figure 1. (a and b) Spin-density patterns (contour value = 0.0025 au) of relaxed the T_1 (^{3}MLCT) triplet state of **1** and **2**, respectively. (c and d) Spin-density patterns (contour value = 0.0025 au) of the relaxed T_1 (^{3}MLCT) and T_2 triplet states of **4**, respectively. (e) Spin-density pattern (contour value = 0.0025 au) of the relaxed T_1 (^{3}MLCT) of **5**.

Table 2. Main Geometrical Features (relaxed structures) Computed for Ground (singlet, S_0) and Lowest-Lying Photoexcited Triplet States (T_1, T_2) of the Various Os(II) Complexes[a]

	1	*[**1**]	**2**	*[**2**]	**4**	*[**4**]		**5**	*[**5**]
	S_0	T_1	S_0	T_1	S_0	T_1	T_2	S_0	T_1
d(M−N_2)	2.066	2.065	2.069	2.072	2.069	2.072	2.069	2.069	2.075
d(M−N_1)	1.988	1.997	1.999	2.026	2.000	2.026	1.999	1.998	1.967
d(M−$N_{2(A)}$)			2.063	2.082	2.063	2.084	2.063	2.063	2.026
d(M−$N_{1(A)}$)			1.979	1.966	1.978	1.967	1.979	1.979	2.026
d(N_{pyr}−C)			1.458	1.458	1.461	1.460	1.458	1.465	1.466
θ_0	30.6	29.2	29.3	28.9	28.7	27.6	29.0	28.4	22.6
θ_{0A}			35.9	36.6	36.7	26.9	36.4	34.0	31.2
θ_1			67.3	66.7	67.7	67.0	67.3	76.4	76.5
θ_2			60.9	59.7	60.4	54.8	61.1	58.6	57.9
θ_6			56.3	59.7	60.4	54.8	61.1	58.6	57.9
θ_4			24.5	25.2	28.0	28.5	21.0	28.9	29.7
θ_{NO2}					0.3	0.5	0.6	0.5	0.5

[a] For nomenclature refer to Chart 2.

(triplet) states (Table 2) for various compounds are compared, the anticipated correlation between structural relaxation and ASP distribution is straightforwardly demonstrated, especially in the case of T_1 within dyads. Thus, it appears that the differential sensitivity of θ_0 and θ_{0A} vis-à-vis planarization, as well as localized degrees of structural rearrangement, can be related to the previously discussed ASP partitioning between the two aryl-tpy ligands (that is aL and L1, respectively) of complex photosensitizers. It is worth bearing in mind, however, that the crucial point for conformational changes is the fact that the spin density encompasses the critical interring bond, regardless of whether the contribution results in a planarization or an increased geometrical decoupling.

No planarization is computed to occur about the intercomponent linkage (θ_1), including in the critical case of conformationally unlocked ***4**, thus showing, once again, *the localized* (P1 or A unit) *nature of the triplet excited states* and further corroborating above-established correlation. Indeed, no (significant) spin density is encountered about the intercomponent bond of the dyads, as can be seen in Figure 1b−e.

3.1.3. Identity of the Novel Triplet State (T_2). A. Dyads 4 and 5. One of the most striking outcomes of the ASP calculations is undoubtedly the existence of a purely ligand-centered (LC) triplet state, T_2, located on the nitro-phenyl (NP) acceptor terminus of **4** (Figure 1d).[48] This ^{3}NP (T_2) state is lying very close in energy to the ^{3}MLCT state (T_1).[1] T_2 has a relaxed geometry very similar to that of the T_1 state, except for θ_{0A} and θ_4 (Table 2). The spin density of T_2 is almost completely located on the nitro group, spreading a little onto the attached phenyl ring and pyridinium fragment. Although rather modest, this spatial extension is sufficient to explain the planarization around θ_4.

We have previously shown that the efficiency of A as an *electron-acceptor*[12,13,22] is closely related to its inner structural features, in particular to θ_1.[1] Apparently, the same does not hold for A when it is considered for its *energy-acceptor*

(48) The existence of an analogous T_2 state for **5** has been confirmed by (vertical) TD-DFT calculations ($\pi-\pi^*$ in nature), but all the attempts to converge this state in a ΔSCF framework were unsuccessful; the T_2 state always relaxes to the more stable and very close in energy T_1 state. Indeed, when the energies (relative to S_0) computed at the TD-DFT level for the T_2 states of both **4** and **5** are compared, in the latter dyads, the T_2 state is found to be slightly more stable (closer to T_1).

properties. This finding is consistent with section 3.1.2, concerning the nature of triplet states, worth considering as locally excited states (LES);[6a] moreover, they are exclusive of the intercomponent linkage. Also, even if the θ_4 angle is found to significantly decrease (by ca. 7°) in **4** on going from the S_0 state to ^{3}NP state, this structural parameter cannot differentiate **4** and **5** because the angle is allowed to relax in the same manner in both species. As a consequence, *the energy gap between the two triplets (T_1 and T_2) should not be related to the intercomponent twist angle* θ_1. T_2 is expected to lie at roughly the same energy within ***4** and ***5**, within ca. 0.16 eV above the corresponding T_1.[48]

The novel NP-centered triplet fulfils the energetic requirements of the experimental study for the postulated equilibrated state (^{3}LC), being *almost isoenergetic* with the relaxed ^{3}MLCT state and preferably *slightly above* it.[1]

Last, on the basis of our calculation for **4**, it is worth noting that the difference in the energy between the *nonrelaxed* (NR) T_2 state (the ^{3}NP state frozen in the geometry of the relaxed ^{3}MLCT state) and the *relaxed* ^{3}MLCT state is extremely small. Therefore, it is not surprising that we were unable to converge the T_2 state of *$[\mathbf{5}]_{NR}$ as the electronic relaxation of the ^{3}NP state systematically results in the close ^{3}MLCT. Thus, in the case of **4**, it is found that relaxation scarcely affects the energy of T_2, which remains roughly isoenergetic with ^{3}MLCT (within 0.16 eV at the maximum).

B. Case of Isolated Nitrobenzene (NB) versus NP within 4 (and 5). Because of the importance of the nitrobenzene-type T_2 state in the photophysical properties of the new Os(II) complexes, one could be tempted to refer to the photophysical behavior of isolated nitrobenzene (**NB**) to interpret the behavior of the dyads. However, from the comparison between the experimental luminescence data for the acceptor models (A_{ref}, Chart 1) reported below (section 3.2) and those of isolated **NB** reported in the literature[49−51] (see also Figure 2), it is apparent that **NB** is actually a poor model for the nitro-containing species studied here.

The luminescence properties of **4** at 77 K are closely related to those of other luminophores of the series, thus clearly indicating that the phosphorescent ^{3}MLCT state is responsible for the emission[1] (see also section 3.1.1). Recovering the sole properties of isolated P1/Os which were lost at room temperature (rt) upon cooling of the sample to low temperature (lt) is indicative of the processes at room temperature being thermally activated. Therefore, in addition to the targeted intramolecular PET process with CS formation (also present in **5**) and postulated equilibration, a supplementary nonradiative deactivation pathway involving the lowest-excited triplet state of the *p*-nitrophenyl moiety (i.e., $^3NP_1 \rightarrow {}^1NP_0$) should also be thermally activated. This behavior is consistent with previous theoretical issues devoted to the bare **NB**.[49b] To account for the very short lifetime

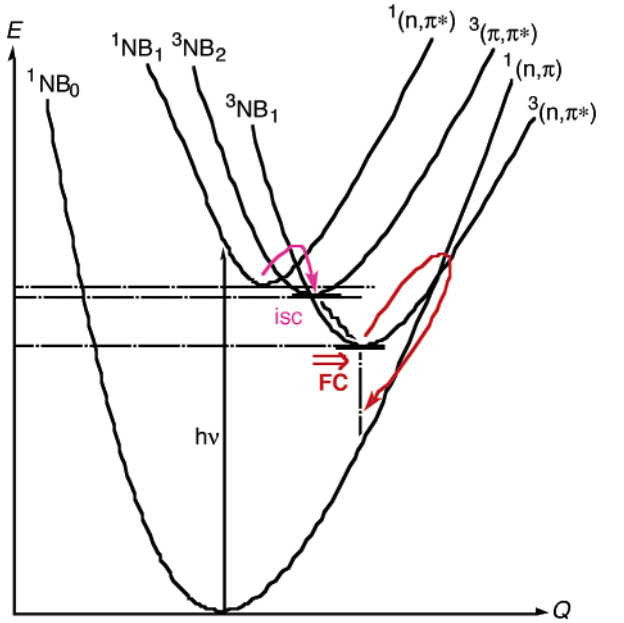

Figure 2. Schematic potential energy diagram for isolated ***NB**.[49−51] Thermally activated nonradiative decay from $^3NB_1$ (red arrow) is favored according to the increase of the Franck−Condon factor (FC).

of the $^1NB_1$ state ($\tau \leq 5$ ps) and related highly efficient $^1NB_1 \rightarrow {}^3NB_1$ apparent intersystem crossing (isc) ($\Phi_{isc} \geq 0.8$) of model **NB**, it was proposed that the isc process actually involves a $^3NB_2$ intermediate state lying close to $^1NB_1$ ($\Delta E(^1NB_1-{}^3NB_2) \approx 0.01-0.03$ eV) that subsequently deactivates to the $^3NB_1$ state (Figure 2). The out-of-plane bending motion of the nitro group was proposed to explain both the very efficient isc and relaxation processes as a large change of geometry between the $^1NB_0$ ground state and the $^1NB_n/^3NB_n$ excited states contributes to an increase the Franck−Condon (FC) factor (see Figure 2).

In contrast, our calculations for TP^+-NO_2 provides values of θ_{NO2} (Table 2) that are about 0.5° (coplanar conformation) for both **4** and **5**.[52] Most importantly, the optimized conformations are found to be *almost the same* for singlet ground states ($^1NP_0$) and excited states, regardless of ^{3}MLCT or $^3NP_1$ triplets being concerned. Such a finding remains valid for calculations performed for corresponding monoreduced complexes including derivatized ligands (see below, section 3.3.2). Hence, the energy of the thermal activation barrier associated with radiationless decay to the ground state is expected to significantly increase accordingly. On this basis, it can be anticipated that, when **NB** is embedded within triarylpyridinio units as in the NP fragment, the related $^3NP_1$ state no longer undergoes fast radiationless decay (see below section 3.2). Therefore, given that the rate of other processes such as fluorescence or charge recombination (CR) from CSS are known to be larger than that of phosphorescence from the present $^3NP_1$ state, the latter could be involved in a reversible electronic EnT equilibrium. This agrees with

(49) (a) Takezaki, M.; Hirota, N.; Terazima, M. *J. Phys. Chem. A* **1997**, *101*, 3443−3448. (b) Takezaki, M.; Hirota, N.; Terazima, M.; Sato, H.; Nakajima, T.; Kato, S. *J. Phys. Chem. A* **1997**, *101*, 5190−5195.
(50) Yip, R. W.; Sharma, D. K.; Giasson, R.; Gravel, D. *J. Phys. Chem.* **1984**, *88*, 5570−5572.
(51) Hurley, R.; Testa, A. C. *J. Am. Chem. Soc.* **1968**, *90*, 1949−1952.

(52) Calculated value of tilt angle θ_{NO2} is significantly different (and lower) from that derived from experimental X-ray crystallography: $\theta_{NO2} = 11.8°$ within **tpy-xy-TPH$_2$(NO$_2$)$^+$**.[1] This discrepancy can be attributed to a known overestimation of the delocalization effects originating from the computational method used (see Ciofini, I.; Adamo, C.; Chermette, H. *J. Chem. Phys.* **2005**, *123*, 121102.).

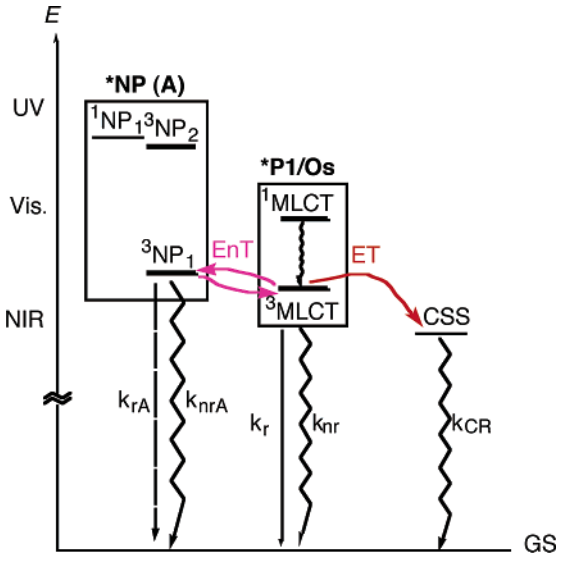

Figure 3. Schematic representation of the interplay of the various triplet states via energy transfer (EnT) processes based on theoretical issues. Electron transfer (ET) process leading to CSS formation is also represented to provide an overall picture (CSS energy level derives from experimental study; see ref 1).

the very long phosphorescence lifetimes of **ph-TPH$_2$(NO$_2$)**$^+$ and **xy-TPH$_2$(NO$_2$)**$^+$ at 77 K (see below).

3.1.4. Model for the Interplay of Triplet States (T_1, T_2) within *4 and *5. The qualitative and schematic energy-level diagram in Figure 3 is based on the following theoretical issues, some of which have already been substantiated at the experimental level:[1]

(i) The ^{3}MLCT level lies at the same energy in the whole series of dyads.[1,53]

(ii) T_1 and T_2 are almost isoenergetic with T_2 lying slightly higher in energy than T_1.[1,53]

(iii) The T_2 lowest-lying LC triplet state involving the nitrophenyl moiety in **4** ($^3NP_1$) is the $^3(n,\pi^*)$ long-lived component of *NP.[48,53]

(iv) The energy of the *NP-centered LES is independent of θ_1 so that energy gap $\Delta E(^3NP_1-{}^3MLCT_1)$ is the same within ***4** and ***5**.[48,53]

(v) The CS state is lying at virtually the same energy within ***4** and ***5**.[1]

(vi) The ^{3}MLCT and ^{3}NP levels are assumed to be similarly affected by temperature.

To build Figure 3, the energy levels were derived from the experimental electronic absorption spectra of dyads **4** and **5**, as well as those of the organic model acceptors, A_{ref} (Chart 1), for the singlet states.[1] These energy levels therefore correspond to nonrelaxed molecular geometry (FC states). Conversely, the energy of the triplets is related to structurally relaxed geometry as it is derived from the emission properties for the ^{3}MLCT level and the computed relaxed triplet T_2 for ^{3}NP.

The photophysical data of the Os(II) complexes are therefore fully rationalized considering that the P1/Os-centered ^{3}MLCT state (T_1) is involved in an equilibration process (reversible electronic EnT) with the close-lying long-lived $^3NP_1$ state, which plays the role of a "small" reservoir of energy.[54] *This equilibration is also in competition with an ET process that involves the same P1/Os-centered ^{3}MLCT level and the TP−NO$_2$ unit as an electron acceptor to form the targeted CS state*.

It is noteworthy that the CS state lies at a significantly lower energy than $^3NP_1$. An estimation of this energy difference can be easily obtained by combining the experimental and theoretical outcomes as the sum of the $^3NP_1-{}^3MLCT_1$ gap (theoretically derived, Table 1) and the $^3MLCT_1-$CSS energy gap derived from experiment.[1] Thus, for **4** we get $\Delta E(^3NP_1-{}^3MLCT_1) + \Delta E(^3MLCT_1-CSS) = 0.160 + 0.125 = 0.285$ eV, so that radiationless decay mediated by NO_2 following intercomponent *ET process* is anticipated to be more efficient accordingly (energy-gap law, EGL).[55] In addition to EGL and the similar (and modest) contribution of the nitro group to the FC factors of molecules in their triplet excited state (see section 3.1.3.A) and "modeled CS state" (i.e., monoreduced species), it is very likely that the FC factor attached to the triplet state (LES in nature) is smaller than that of the more *delocalized* CSS state (see section 3.3.1), thus speeding up the radiationless decay from CSS accordingly.

3.2. Experimental Validation of the Theoretical Issues: Photophysical Insights. The photophysical behavior of **4** (and **5**) is directly related to the interplay between the intraligand *p*-nitrophenyl-centered triplet state T_2 ($^3NP_1$, theoretically shown) and the photosensitizer-centered triplet state T_1 (^{3}MLCT, both experimentally[1] and theoretically[53] shown). A reversible electronic energy exchange (equilibration process) is indeed expected because these triplets coexist within a narrow range of energy.

To corroborate computational issues, one can perform the following experiments, based on the LES nature, established in this work, for triplets T_1 and T_2.

First, one can reasonably expect that the photophysical behavior of the **ph-TPH$_2$(NO$_2$)**$^+$ and **xy-TPH$_2$(NO$_2$)**$^+$ organic molecules (Chart 1) accurately reproduce the photophysical features of the ^{3}NP states in **4** and **5**, respectively. To better clarify the roles of the R^0 methyl substituents (conformational locking) and nitro group, it's therefore of interest to investigate the luminescence properties (at both 298 and 77 K) of the series of organic reference molecules A_{ref} (Chart 1), including those of the nonderivatized **ph-TPH$_3$**$^+$ and **xy-TPH$_3$**$^+$ acceptor models.

Second, we know that the ^{3}MLCT excited-state of P1 in **4** (P1/Os) is lying at lower energy than that of P1 in the ruthenium analogue (P1/Ru, **9**) (by ca. 0.21 eV at 77 K).[1] At the same time, the LC triplet state (^{3}NP) is theoretically postulated to lie at the same energy in both dyads. Therefore, it is worth studying the effect of a change in the energy gap between the ^{3}MLCT and ^{3}NP levels upon equilibration via a comparison of the photophysical behavior of **9** and **4**, as well as that of **10** and **5**.

(53) This work.

(54) Passalacqua, R.; Loiseau, F.; Campagna, S.; Fang, Y.-Q.; Hanan, G. S. *Angew. Chem., Int. Ed.* **2003**, *42*, 1608−1611.

(55) Assuming the same geometry for the *NP luminophore fragment.

Table 3. Photophysical Properties (Fl, fluorescence; Ph, phosphorescence, λ/nm) of Reference Model Acceptors and P1 Luminophores Embedded within Selected Ru(II)- and Os(II)-Based Dyads at Both Room Temperature (rt) and 77 K (lt)[a]

					P1-A/NO_2		P1/Me2-A/NO_2	
	ph-TPH$_3^+$	**xy-TPH$_3^+$**	**ph-TPH$_2$(NO$_2$)$^+$**	**xy-TPH$_2$(NO$_2$)$^+$**	**9**/Ru	**4**/Os	**10**/Ru	**5**/Os
λ_{Fl} (rt)	480	458	495	468				
τ_{Fl} (rt), ns	3.0	18.6	3.8	4.8				
λ_{Ph} (rt)	nd	nd	nd	nd	676	745	674	743.5
τ_{Ph} (rt), ns	nd	nd	nd	nd	7	174	1	0.87
λ_{Fl} (lt)	390	389	365	369				
τ_{Fl} (lt), ns	5.1	5.7	0.20	0.15				
λ_{Ph} (lt)	450	446	726	728	645	725	637	729
τ_{Ph} (lt), μs	107 000	127 000	5100	4900	10.0	3.09	12.5	3.20

[a] nd = not detected.

The results of the specific photophysical study are collected in Table 3.

As is generally the case for purely organic luminophores, the fluorescence emission dominates the phosphorescence emission at room temperature because of the much higher sensitivity of the latter process to solvent reorganization.

When analyzing the data collected in Table 3, one can distinguish between photophysical outcomes concerning A_{ref} organic luminophores as a function of temperature. At first glance, at room temperature, **ph-TPH$_3^+$** behaves like **ph-TPH$_2$(NO$_2$)$^+$**, whereas **xy-TPH$_3^+$** behaves like **xy-TPH$_2$(NO$_2$)$^+$**. Conversely, at lt, **ph-TPH$_3^+$** behaves like **xy-TPH$_3^+$**, while **ph-TPH$_2$(NO$_2$)$^+$** behaves like **xy-TPH$_2$(NO$_2$)$^+$**. These different behaviors can be interpreted as follows.

(i) The behavior at lt is fully consistent with the presently reported theoretical issues related to the $^3NP_1$ state of nitro derivatives. Most importantly, the statement regarding the independence of the triplet energy levels from the θ_1 twist angle is confirmed, meaning that the $^3NP_1$ state lies at the same energy (ca. 1.705 eV/$\lambda_{em} \approx$ 727 nm on average) regardless of whether **4** or **5** (**ph-TPH$_2$(NO$_2$)$^+$** or **xy-TPH$_2$(NO$_2$)$^+$**, respectively) is concerned. This finding further corroborates that T_1 and T_2 are LES in nature. Experimental data also confirm the existence of a strongly phosphorescent state in the visible region (ca. 2.768 eV/$\lambda_{em} \approx$ 448 nm on average) previously mentioned in the literature.[13] This state can be straightforwardly attributed to a pyridinium-centered triplet ($^3Py_1$), clearly different from other $^3NP_1$ LES. Fluorescence emission at lt discloses singlet energy levels corresponding to above-identified NP- and Py-centered triplets. $^1NP_1$ is found to lie at ca. 3.379 eV on average ($\lambda_{em} \approx$ 367 nm), not far from $^1Py_1$: ca. 3.184 eV ($\lambda_{em.} \approx$ 390 nm).

The fact that emission from the $^3NP_1$ state (phosphorescence) is found to be very close (*isoenergetic* within the experimental error) to that originating from the ^{3}MLCT of *P1/Os in both **4** and **5** is also of paramount importance. Conversely, for Ru-based species **9** and **10**, the energy gap between $^3NP_1$ and $^3MLCT_1$ is too large (ca. 0.22 eV) to allow equilibration. As already discussed, the photophysical behavior of ***NB**[49−51] is sharply different from that of the closely affiliated NP fragment (Table 3). This discrepancy can be attributed to the presence of a linked electron-withdrawing pyridinium.

(ii) For the photophysical behavior at room temperature, the most striking feature is the very large Stokes shift of ca. 1.45 eV on average, seen in the fluorescence emission of all four A_{ref} species (given a LC absorption at ca. 305 nm).[1] This is indicative of a huge structural reorganization upon photoexcitation. Another salient feature is that the emission energy is apparently no longer determined by the presence of the nitro group (as is the case at 77 K), but it is sensitive to the θ_1 twist angle instead, in relation to the presence of R^0 methyl substituents on the *N*-pyridinio moiety.

Basically, these two findings are closely related and consistent with a delocalized description of the emissive singlet states for the entire triarylpyridinium series, including the *N*-pyridinio aryl substituent. The emission at room temperature is therefore worth considered as originating from a unique $^1[pTP]_1$ singlet state for the whole series, lying at ca. 2.278 eV ($\lambda_{em.} \approx$ 463 nm) and 2.543 eV ($\lambda_{em.} \approx$ 488 nm) on average within conformationally locked and unlocked luminophores, respectively.

As a matter of fact, the theoretical issues (summarized in Figure 3) are in full agreement with the insights gained from present lt photophysical behavior of the A_{ref} series. Therefore, a description of photoinduced processes derived from the combined computational and experimental outcomes can now be proposed (Figure 4) that accurately accounts for the observed photophysical behavior[1] of the Os-based dyads **4** and **5**, as well as the Ru-based analogues (**9** and **10**), at both rt and lt.

For the electronic EnT, it appears that the Coulombic Förster mechanism[56] can be ruled out because the donor, D (P1/Os), is a red emitter while the acceptor, A (TP-NO_2^+), is a UV absorber. EnT is preferably based on an exchange interaction of the Dexter type,[57] mediated by orbital overlap between P1 and A, supported by Ph[1]. As expected, this is a thermally activated process,[58] and it was found to be precluded at low temperature (cf. Table 3),[1] as is the case for the ET processes when they are not exceedingly exergonic. However, even more than ET, Dexter EnT is very sensitive to the nature of the bridging element that mediates the electronic coupling between D and A.[15a,19] Ceteris paribus, the loss of conjugation (about θ_1) within geometrically *constrained* (even locked) **5** as compared to *restrained* **4** (allowed to probe a wider range of conformations about the mean θ_1 angle thanks to thermal structure fluctuations)[1] appears to be sufficient to preclude[59] an energy

(56) Förster, Th. *Discuss. Faraday Soc.* **1959**, *27*, 7−17.
(57) Dexter, D. L. *J. Chem. Phys.* **1953**, *21*, 836−850.
(58) Ryu, C. K.; Schmehl, R. H. *J. Phys. Chem.* **1989**, *93*, 7961−7966.

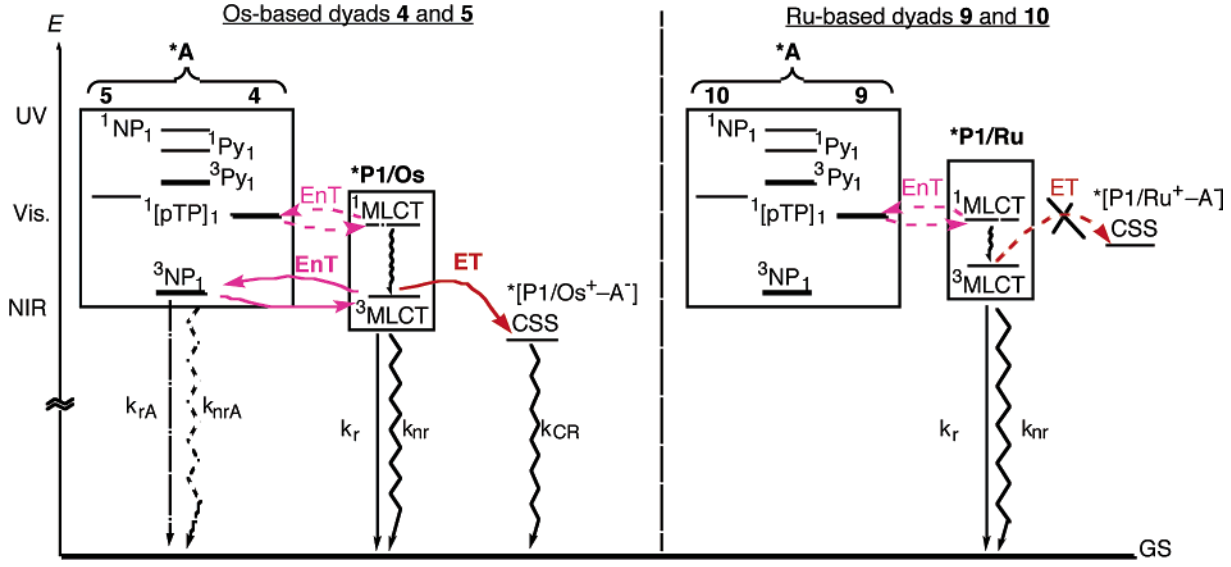

Figure 4. Schematic energy level diagrams accounting for room temperature and lt behavior of Os- and Ru-based dyads, derived from cross theoretical and experimental (*emission*) outcomes. All identified LC singlet states are shown, although not present at the same temperature (see text). The ^{1}MLCT state lies at the same energy in Os- and Ru-based dyads as determined by electronic *absorption* (ca. 491 nm/2.52 eV).[1] Dashed arrows indicate ineffective processes.

equilibrium based on the ^{3}NP$_1$ and ^{3}MLCT$_1$ states.[15a,19] Moreover, as is the case for **2**,[12b] one can reasonably state that both of **4** and **5** adopt the same, more stable, axially distorted geometry close to that of **5** in the ground state[1] regardless of whether the molecules are in fluid solution or in frozen matrix. However, contrary to the θ_{0A} and θ_0 twist angles showing that they have room for planarization in the the excited state in a rigid matrix,[1] conformational motion about the θ_1 torsion angle can be ruled out because of the great steric hindrance[60] of TP$^+$ molecular fragment.

As can be seen in the schematic energy-level diagram of the Os-based dyads (Figure 4), another equilibration process is a priori expected to occur within **4** at room temperature (as well as in **9**, for the Ru-based analogue), involving ^{1}pTP$_1$ and ^{1}MLCT *singlet* states. However, when the equilibration rate (2×10^9 s^{-1}) established for a similar process based on triplet states[1] is compared with the high efficiency rate ($\Phi_{isc} \approx 1$)[61] of the deactivation isc process (ca. 3.3×10^{12} s^{-1})[45] of the ^{1}MLCT$_1$ state, it appears that this supplementary equilibrium has no time to fully develop, and it is not detected accordingly[1] especially because equilibration based on lowest-lying levels (triplets) is present in the case of **4**. The contribution of equilibration relying on singlets is therefore negligible.

3.3. Later Stages of Photoinduced Charge Transfer: Intercomponent ET Processes. 3.3.1. Electronic Redistribution: CSS Formation. Metal-to-ligand charge-transfer electronic transitions can be considered to be light-triggered intramolecular redox reactions where the metal center is oxidized while the ligands are reduced.[60] As we are mainly interested in understanding the photoexcited states where an electron is promoted on the ligands embedded within complexes, a fruitful approach is to simulate the behavior of the monoreduced species[13,22,60,62] because reduction is known to be essentially a ligand-centered process.[61] This statement is even more pertinent in the case of an intercomponent ET, which can be viewed as a borderline case of an outer-sphere ET process between the primary donor (*P1) and the acceptor, no longer being limited by diffusion because A is docked with P1 via a covalent bond. The spin-density distribution calculated for the monoreduced dyads are collected in Table 4.

Table 4. Computed ASP Distributions for the Relaxed Ground State of Various Os(II) Complexes in Their Reduced Forms (in fraction of electron; sum = 1) Including Hypothetical [**4** + 2Me]$^-$ and [**5** − 2Me]$^-$ Species (see text, section 3.3.3) Frozen in the Relaxed Geometry of Reduced Parent Dyads (**4** and **5**, respectively)

	[**1**]$^-$	[**2**]$^-$	[**4**]$^-$	[**4** + 2Me]$^-$ (S_0 reduced)	[**5** − 2Me]$^-$ (S_0 reduced)	[**5**]$^-$
Os	**0.028**	**0.126**	**0.110**	**0.106**	**0.116**	**0.110**
tpy$_A$	0.460 × 2	0.720	0.560	0.520	0.641	0.620
Ph^1/Xy	0.026 × 2	0.080	0.090	0.070	0.083	0.060
L1	**0.486 × 2**	**0.800**	**0.650**	**0.590**	**0.724**	**0.680**
pyridinium		0.050	0.180	0.237	0.120	0.160
Ph^4		0.006	0.040	0.025	0.017	0.020
NO_2			0.010	0.015	0.010	0.010
A		**0.074**	**0.230**	**0.277**	**0.156**	**0.190**
aL		**0.000**	**0.010**	**0.027**	**0.004**	**0.020**

The main outcomes for the monoreduced complexes determined via the theoretical analysis are the following:

(i) The ASP corresponding to the unpaired electron located on the NO_2 group is computed to represent only 5% of total ASP distributed on the acceptor. Such a low contribution suggests a strong electronic delocalization over the entire A component, as inferred from the experimental study.[1] Thus, it also demonstrates that a small contribution may result in

(59) Actually, the decreased rate for the reversible electronic EnT in **5**, as compared to **4**, makes energy equilibration to be no longer competitive with faster intercomponent ET leading to CSS formation, so that the EnT process does not occur (see ref 1).

(60) McCusker, J. K. *Acc. Chem. Res.* **2003**, *36*, 876−887.
(61) Juris, A.; Balzani, V.; Barigelletti, F.; Campagna, S.; Belser, P.; Von Zelewsky, A. *Coord. Chem. Rev.* **1988**, *84*, 85−277.
(62) Gabrielsson, A.; Matousek, P.; Towrie, M.; Hartl, F.; Zalis, S.; Vlcek, A., Jr. *J. Phys. Chem. A* **2005**, *109*, 6147−6153.

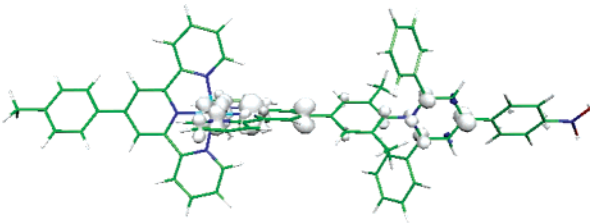

Figure 5. Spin-density pattern of the reduced **5** (contour value = 0.0025 au).

Table 5. Computed ASP Distributions for the Ground State of Various Reduced Ligands (in fraction of electron, sum = 1) in Their Relaxed Geometry[a]

	$[L1\text{-}A]^-$	$[L1\text{-}A/NO_2]^-$	$[L1/Me2\text{-}A/NO_2]^-$
tpy_A	0.017	0.004	0.001
Ph^1/Xy	0.023	0.022	0.000
L1	**0.040**	**0.026**	**0.001**
pyridinium	0.883	0.638	0.631
Ph^4	0.015	0.082	0.190
NO_2		0.132	0.139
A	**0.960**	**0.974**	**0.999**

[a] cf Figures SI1a−c (Supporting Information).

large spectroscopic effects[41b,63] because NO_2 is very likely to be largely responsible for the fast decay of CSS (CR process).[1]

(ii) Upon going from $[\mathbf{2}]^-$ to nitro derivatives $[\mathbf{4}]^-$ and $[\mathbf{5}]^-$, the spin density on A is increased at least three times, while that located on L1 is decreased by ca. 17%.

Significant differences can be observed when the ASP values calculated for reduced species **4** and **5** (Figure 5) are compared with those of the relaxed triplet states (Figures 1c−e), especially for the spatial expanse of the spin-density distribution. Also, dependent on if A is considered for its energy- or electron-accepting properties, the related relevant spin density is mainly located at the NP terminus (LC T_2) or about the pyridinium core, respectively.

Part of the contribution of the coordinated positively charged metal cation toward the spin-density redistribution can be inferred from a comparison of the computed ASP partition for isolated (free) reduced ligands (Table 5) with data for the complexes (Table 4). The metal dication is found to withdraw spin density initially located on the acceptor moiety (in the free ligands) for the Ph^1 and tpy_A fragments of L1 (in complexes). Therefore, in genuine photoproduced CT states, where the electron promoted on the derivatized ligand originates from the metal center, the observed propensity is anticipated to be enhanced accordingly. To some extent, this statement can be partly verified when looking at the ASP partitions within T_1 triplet states of **4** and **5** (Table 1).

3.3.2. Structural Reorganization upon ET: Planarization of the CS States. To better characterize the anticipated changes of intramolecular geometry upon reduction, structure optimizations have been performed for complexes **1**, **2**, **4**, and **5** in both their native and monoreduced forms (Table 6).

(63) Rack, J. J.; Winkler, J. R.; Gray, H. B. *J. Am. Chem. Soc.* **2001**, *123*, 2432−2433.

Table 6. Main Structural Features Computed for the Relaxed Ground States of the Os(II) Complexes in Both Their Native[a] and Monoreduced Forms

	1	$[\mathbf{1}]^-$	**2**	$[\mathbf{2}]^-$	**4**	$[\mathbf{4}]^-$	**5**	$[\mathbf{5}]^-$
$d(M-N_2)$	2.066	2.065	2.069	2.057	2.069	2.059	2.069	2.058
$d(M-N_1)$	1.988	1.981	1.999	1.969	2.000	1.974	1.998	1.973
$d(M-N_{2(A)})$			2.063	2.063	2.063	2.064	2.063	2.062
$d(M-N_{1(A)})$			1.979	2.002	1.978	2.000	1.979	2.001
$d(N_{pyr}-C)$			1.458	1.455	1.461	1.448	1.465	1.458
θ_0	30.6	32.7	29.3	33.1	28.7	32.0	28.4	31.8
θ_{0A}			35.9	26.3	36.7	23.4	34.0	29.5
θ_1			67.3	64.1	67.7	58.6	76.4	73.9
θ_2			60.9	53.6	60.4	56.5	58.6	49.9
θ_6			56.3	57.1	60.4	56.5	58.6	54.6
θ_4			24.5	26.8	28.0	27.0	28.9	27.4
θ_{NO2}					0.3	0.6	0.5	0.5

[a] Structural features of relaxed ground states (Table 2) are reported again for comparison purposes.

When analyzing Table 6 and, more specifically, the dihedral angle changes upon reduction, one can observe two types of planarization effects.

On one hand, there is the relaxation internal to the P1/Os photosensitizer (θ_0, θ_{0A}) detected by ultrafast spectroscopy.[1] Here, in contrast to the results obtained for the triplet states (Table 2), this planarization appears to always concern the aryl-tpy ligand bearing the acceptor. The decrease of θ_{0A} is found to be systematically (only partially) compensated by a slight increase of θ_0. As expected, the larger modification occurs within $[\mathbf{4}]^-$ ($\Delta\theta_{0A} = 13.3°$).

On the other hand, there is a decrease of the critical torsion angle (θ_1) controlling the conjugation of L1 (and P1/Os) with A. The largest modification occurs in $[\mathbf{4}]^-$ ($\Delta\theta_1 = 9.1°$), while the smallest appears in $[\mathbf{5}]^-$ ($\Delta\theta_1 = 2.5°$) because of steric encumbrance. Accordingly, in $[\mathbf{4}]^-$, the intercomponent linkage ($d(N_{pyr}-C)$) is found to be shortened more significantly (down to 1.448 Å), upon reduction, than that in the other reduced dyads (down to 1.456 Å, on average). This type of planarization was not calculated for the triplet LES and actually reveals the *extended nature of the CS states*.

To get a more complete picture of structural reorganization upon reduction, the geometry has also been optimized for the reduced free ligands (Table 7).

The main outcome of these calculations stems from the fact that a third type of planarization effect is found to occur, namely, the intra-acceptor relaxation about θ_4, anticipated in the experimental study[1,64] and shown in the investigation of the triplet states (Tables 1 and 2). As a matter of fact, the most pronounced intra-acceptor planarization effect of the whole series is found for $[L1/Me2\text{-}A/NO_2]^-$: θ_4 is decreased by ca. 27.5 ° to become 3.0°.

Apparently, our calculations are in better agreement with the experimental data for the reduced species than for the

(64) As is the case for the ^{3}MLCT state and other CT states,[26−32] one can anticipate that the transiently reduced acceptor undergoes a structural relaxation, independent of the yet planarized aryl-tpy moiety of the P1/Os luminophore. Planarization is expected because the acceptor part, which mainly consists of a pyridinium ring and a terminal phenyl with a conjugated nitro substituent (π-extending group likely to favor a quinoidal structure), is already nearly planar in the ground state,[1] as is the case for ph-tpy ligand ($\theta_0 \approx 25°$)[12b] within P1/M. In addition, the lifetime of the CT (CS) state is long enough to allow the few-picosecond planarization to take place.[1]

Table 7. Main Structural Features Computed for the Relaxed Geometry of Various Ligands in Both Their Native and Reduced Forms

	L1-A	$[L1\text{-}A]^-$	L1-A/NO_2	$[L1\text{-}A/NO_2]^-$	L1/Me2-A/NO_2	$[L1/Me2\text{-}A/NO_2]^-$
$d(N_{pyr}-C)$	1.461	1.431	1.463	1.447	1.463	1.447
θ_{0A}	30.8	27.6	31.7	30.25	31.27	28.97
θ_1	66.7	54.3	66.8	60.22	66.80	73.93
θ_2	56.7	50.2	56.0	54.04	56.02	53.27
θ_6	56.7	50.2	56.0	54.04	56.02	53.27
θ_4	27.0	14.7	30.7	8.06	30.6	3.0
θ_{NO2}			0.1	0.2	0.2	0.0

excited triplets. This behavior is strictly related to the fact that the electronic configurations of the reduced systems are well defined (an unpaired electron in the *unique* SOMO), whereas the different triplet states may be close in energy and, therefore, in competition. In this latter case, the experimental observation is an average over the different electronic configurations and the resulting structural effects are generally less pronounced. In short, our results confirm that the CT states are correctly modeled from the viewpoint of their electronic features by computing the corresponding monoreduced species,[22,60] but they also demonstrate that the same holds *for structural relaxation* within the Ru/Os oligopyridine complexes.

Of note, also, is the fact that no planarization is observed in the case of symmetrical $[\mathbf{1}]^-$, but a slightly opposite propensity is seen instead. A possible explanation stems in the fact that structural relaxation is usually the consequence of electronic redistribution within a polarized structure (of push−pull type). In the whole series, except **1**, the molecules are polar in nature because of the presence of an acceptor group (dyads). The planarization, experimentally shown in the case of *[**1**],[1] very likely originates from a symmetry breakdown related to a primary electron transfer from the metal center to *one of the two* ttpy ligands. Indeed, *[**1**] does exhibit substantial third-order nonlinear optical activity.[65] In our calculation, the molecule is symmetric so that polarization is consequently withdrawn. To solve this problem, one could introduce a symmetry breakdown (at the geometrical level) for the molecule in the excited state and subsequently perform electronic and structural relaxation.

3.3.3. Roles of R^0 substituents. The following features reveal the structural effects of R^0 methyl substituents:

(i) For the relaxed triplet states, the lengthening of $d(N_{pyr}-C)$ intercomponent bond within **5** (1.465 Å) as compared to other dyads (1.458 Å, see Table 2) is one effect. The same trend is observed for native ground states and is actually correlated with the decrease in the intercomponent degree of conjugation caused by increased geometrical decoupling (Table 6).

(ii) The θ_1 angle is systematically larger (by ca. 10°) and closer to 90° in **5** than in the other dyads, in both the ground singlet and the excited triplet states (Table 2). This point is even more important because there is a propensity of the molecules to get more flattened upon reduction (Table 6). As expected, the flattening is much less pronounced within **5**.

The effects of structural relaxation upon the distribution of spin density corresponding to unpaired electron (MLCT triplet state or monoreduced species) is also evident when the ASP patterns for the nonrelaxed and corresponding optimized (i.e., relaxed) structures of **1** and **2** (see Supporting Information, Table SI-1) are compared.

In addition to the geometrical effects, the electronic (inductive) contribution of the two methyl (Me) groups R^0 has been assessed. Thus, the spin-density redistribution within hypothetical $[\mathbf{4} + 2Me]^-$ and $[\mathbf{5} - 2Me]^-$ monoreduced species frozen in the relaxed geometry of reduced parent dyads (**4** and **5**, respectively) have been computed. By comparing reduced dyads with and without R^0 substituents (Table 4), we found that the presence of the methyl groups results in a decrease of the spin density on the L1 moiety (by ca. 6.8% on average) and on the xylyl spacer (by ca. 25% on average). A similar trend has already been shown in section 3.1.1 for the computed spin-density partitioning of triplet MLCT (T_1) within various photoexcited dyads.

With all these data taken together, it is found that the R^0 substituents do play a determining role at both the *structural* and *electronic* levels, as further shown when the computational issues concerning the reduced free ligands are examined (Tables 5 and 7). Hence, the spin density corresponding to the odd electron is found to be almost completely (up to 99.9%) localized on the acceptor moiety within $[L1/Me2\text{-}A/NO_2]^-$, while a certain degree of back charge transfer toward the L1 fragment is noticed for other ligands.

3.3.4. Interplay between the EnT and ET Processes within 4 and 5. The photophysical behavior of **4** and **5** osmium(II) dyads is schematically summarized in Figure 6.

For **5**, the driving force for the CS formation (i.e., the energy difference between the ^{3}MLCT and CS states) is slightly larger than that for **4**, and at the same time, partial interplane conjugation is precluded by steric hindrance about θ_1. Both factors contribute to prevent the occurrence of *an easy reversible* EnT process, which basically corresponds to a double-electron exchange, to the advantage of a fully developed CS and fast CR, as shown by the photophysical properties of **5**.

For both **4** and **5** dyads, the fact that reduction of A is postulated to result in a planarization about θ_4 is accompanied by a correlated increase of the acceptor strength of A[31,66] which further lowers the energy level of CSS and speeds CR, accordingly.

(65) Konstantaki, M.; Koudoumas, E.; Couris, S.; Lainé, P.; Amouyal, E.; Leach, S. *J. Phys. Chem. B* **2001**, *105*, 10797−10804.

(66) Beer, P. D.; Chen, Z.; Grieve, A.; Haggitt, J. *J. Chem. Soc., Chem. Commun*. **1994**, 2413−2414.

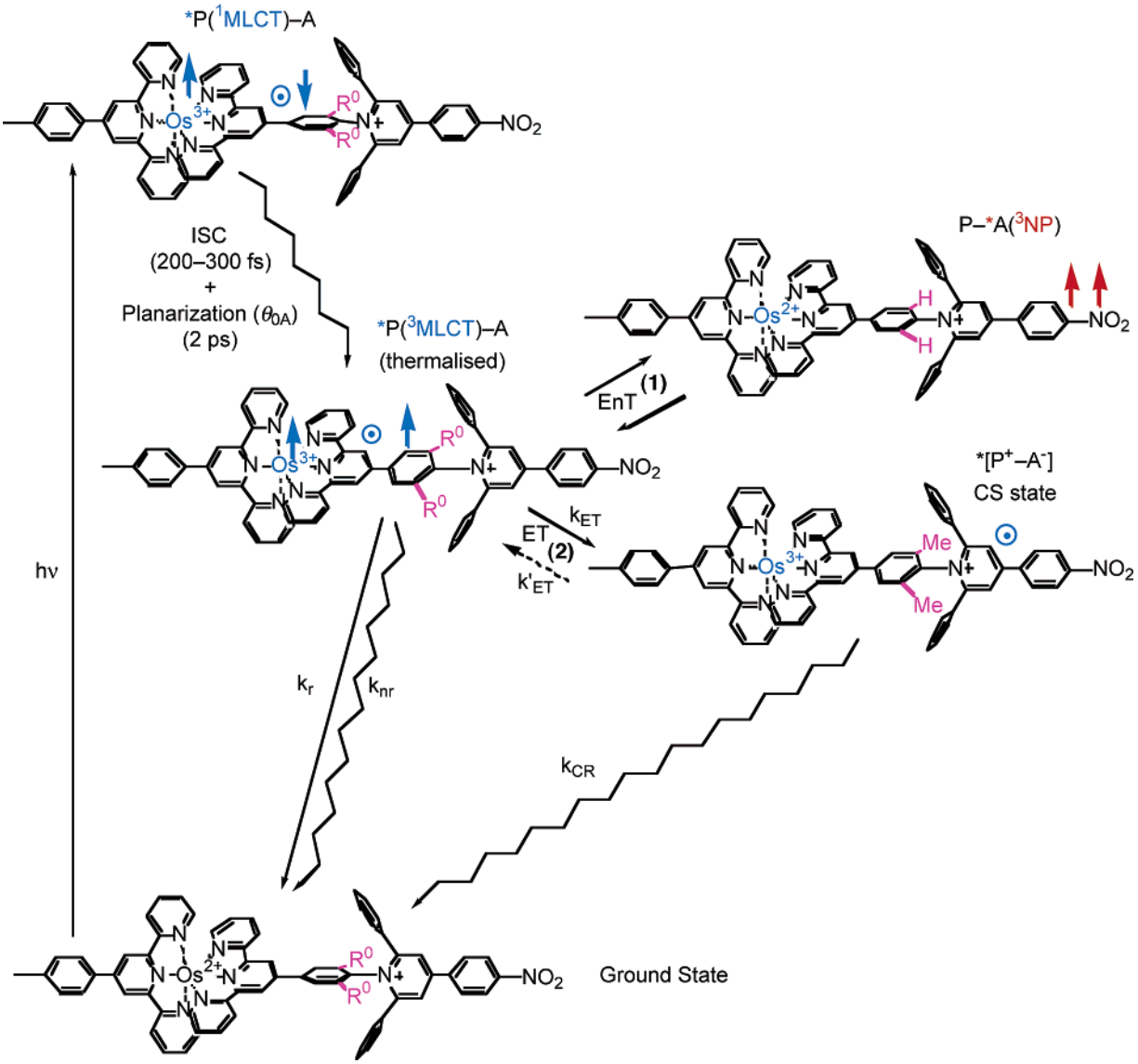

Figure 6. ET and EnT processes within **4** and **5**. In the case of **5**, channel 1 is not operative as P-*A($^3NP_1$) and *P($^3MLCT_1$)-A LES are not sufficiently coupled because of an almost complete loss of intercomponent conjugation.

Finally, for the interplay between ET and EnT, a possible feedback effect of planarization about the NP moiety (T_2 formation within A upon equilibration) on the efficiency of intramolecular ET (and CSS formation) within **4** cannot be ruled out.

4. General Comments

An accurate description of the electronic/spin properties of the reduced species requires a structure optimization, even if spectroscopic signatures could be barely affected by structural modifications.[22] The computational outcomes for the spin-density maps are also strongly different depending on whether relaxed triplet states (Table 1) or relaxed ground states for reduced species (Tables 4 and 5) are considered. Assuredly, it is worth referring to the latter to rationalize the consequences of intramolecular ET and structure relaxation. The computed patterns are in agreement with our expectations both for the free ligands and related complexes. Therefore, computing the features of the monoreduced species is a fruitful strategy, especially for modeling the structural relaxation (planarization effect) of CT (including CS) states.

The sizable planarization upon CT inferred from the experimental study[1] is well supported by the theoretical calculations. This structural relaxation has been found at the theoretical level for other states, such as CS and ^{3}LC. It is worth taking into account the excited-state geometrical changes even in semirigid architectures, especially because the supermolecules are potentially fully conjugated and there is room for intramolecular torsional motion (as in the case of **4**). Indeed, changes of the conformation upon excitation can therefore have important consequences, namely, fluctuations of critical intercomponent electronic coupling,[33] which can explain the occurrence or not of electronic energy exchange (equilibration) within ***4** and ***5**, respectively.

The calculations further confirm the existence of the interplay between the P and A subunits, previously inferred from theoretical[22] and experimental[1,12,13] studies, mediated

by the *N*-pyridinio bridging element (B). To some extent, we are here in the case of quite closely coupled systems (so-called "compact dyads")[13] because of non-negligible intercomponent electronic coupling, as is the case, for instance, for the recently reported P0/Ru-pym-An dyads,[54] where pym is a pyrimidyl fragment to be likened to Ph^1 (B) and An is an anthracene *energy* acceptor (TP^+ can also be this).

Calculation of the excited triplet states for the various dyad species allowed the nature of the "equilibrated triplet state" to be identified, the existence of which was postulated from experimental results in the experimental part of the study.[1] Indeed, the involvement of an intraligand NP-centered triplet state (^{3}NP) in a reversible electronic EnT with the P1/Os-centered ^{3}MLCT state within **4** was confirmed by performing complementary photophysical investigations (Table 3) on model acceptor species (A_{ref}, Chart 1).

R^0 substituents were shown to fulfill their role regarding excited-state torsional motion about the intercomponent linkage (θ_1) within **5** regardless of whether fluctuations are of thermal origin (case of triplet LES for reversible EnT) or are from the ensuing charge redistribution (as in the case of the spatially extended CS states). Indeed, the *constraining* methyl groups were found to prevent the −xylyl− spacer and the pyridinium ring from adopting a more flattened conformation, which is partially allowed within *restrained* **4** in the excited state. Interestingly, these substituents were also shown to contribute to reinforcing of the intercomponent decoupling at the electronic level thanks to their inductive electron-donating properties via polarization effects. *Actually, the combined structural and electronic contributions of the R^0 methyl substituents are found to be determining for the occurrence of the equilibration process, and this explains why **4** and **5** behave differently*.

Last, the spin-density calculations further substantiate the formation of the CS state within photoexcited **4** and **5** osmium(II) dyads postulated on the basis of experimental outcomes.[1] The appending of an electron-withdrawing group, such as NO_2, has substantial consequences on the electronic distribution, even in the case of a residual intercomponent (L1−A) conjugation. This result further substantiates our engineering approach, even if NO_2 is not the best candidate from a spectroscopic viewpoint.[62]

5. Concluding Remarks

The interplay between theory and experiment has been proven to be a powerful tool for the investigation of complex molecular systems. In particular, we have shown that the electronic and structural reorganization occurring during photoinduced processes can now be analyzed and rationalized using ab initio approaches based on density functional theory.

This study allowed us to gain insights into excited-state intramolecular upheaval within widely used ph-tpy-based photosensitizers.[9] These issues can straightforwardly be extrapolated to other complexes of aryl-substituted oligopyridyl ligands, ubiquitous throughout many fields of modern inorganic chemistry.[2a,61,67] They prepare a new ground for the engineering of excited states, which is of pivotal importance when designing PMDs.

For the dyads analyzed, we have also provided clear evidence of the existence of a switching effect based on the conformational gating of intramolecular photoinduced processes.

Present-day conjunction[46,60,68] of advanced time-resolved spectroscopies[69,70] and theoretical tools[71,72] allows one to clearly define the interplay between electronic and geometrical structures *even in the excited state*, so that integration of the *electronic coupling* as a *full functional ingredient* of future PMDs can now be envisioned.[13,54,73] The ultimate goal is to take advantage of close and cross-functional interactions to make it possible to exceed synergetic functioning of PMDs and reach an even symbiotic (nonlinear) manner of behaving. In other words, as the diversity produced within the intramolecular landscape is becoming sufficient, the whole idea is now to seek for possible light-induced functional *emergences*[74,75] within a new kind of closely coupled (compact)[13] PMDs.

Acknowledgment. The authors thank Dr. F. Bedioui for stimulating discussions. C.A. and I.C. are grateful to the Institut de Développement et Ressources en Informatique Scientifique (IDRIS, Orsay) for a generous allocation of computer time (Project 05173), and P.P.L. is thankful to the French Ministry of Research for financial support (ACI Project JC4123). S.C. also acknowledges MIUR (FIRB and PRIN projects) for funding.

Supporting Information Available: Computed ASP for the triplet state of various native Os(II) complexes (excited states), together with that for their reduced forms in the ground state, and HOMO and LUMO of the relaxed L1-A/NO_2 ligand, together with the spin-density pattern for the SOMO of the relaxed [L1-A/NO_2]$^-$ reduced ligand This material is available free of charge via the Internet at http://pubs.acs.org.

IC060679T

(67) (a) Hofmeier, H.; Schubert, U. S. *Chem. Soc. Rev.* **2004**, *33*, 373−399. (b) Andres, P. R.; Schubert, U. S. *Adv. Mater.* **2004**, *16*, 1043−1068.
(68) Browne, W. R.; O'Boyle, N. M.; McGarvey, J. J.; Vos, J. G. *Chem. Soc. Rev.* **2005**, *34*, 641−663.
(69) Special Issue on Femtochemistry. *Chem. Rev.* **2004**, *104*, 1717−2124.
(70) Vlcek, A., Jr.; Farrell, I. R.; Liard, D. J.; Matousek, P.; Towrie, M.; Parker, A. W.; Grills, D. C.; George, M. W. *J. Chem. Soc., Dalton Trans.* **2002**, 701−712.
(71) Dreuw, A.; Head-Gordon, M. *Chem. Rev.* **2005**, *105*, 4009−4037.
(72) Martinez, T. J. *Acc. Chem. Res.* **2006**, *39*, 119−126.
(73) Ziessel, R.; Bäuerle, P.; Ammann, M.; Barbieri, A.; Barigelletti, F. *Chem. Commun.* **2005**, 802−804.
(74) Müller, A.; Reuter, H.; Dillinger, S. *Angew. Chem., Int. Ed. Engl.* **1995**, *34*, 2328−2361.
(75) Whitesides, G. M.; Grzybowski, B. *Science* **2002**, *295*, 2418−2421.